

Repeatability of Dixon magnetic resonance imaging and magnetic resonance spectroscopy for quantitative muscle fat assessments in the thigh

Alexandra Grimm^{1*}, Heiko Meyer², Marcel D. Nickel², Mathias Nittka², Esther Raithe², Oliver Chaudry¹, Andreas Friedberger¹, Michael Uder³, Wolfgang Kemmler¹, Klaus Engelke^{1,4} & Harald H. Quick^{1,5,6}

¹Institute of Medical Physics, Friedrich-Alexander-Universität Erlangen-Nürnberg (FAU), Henkestr. 91, Erlangen 91052, Germany, ²Diagnostic Imaging, Magnetic Resonance, Product Definition and Innovation, Siemens Healthcare GmbH, Allee am Roethelheimpark 2, Erlangen 91052, Germany, ³Institute of Radiology, University Hospital Erlangen, Ulmenweg 18, Erlangen 91052, Germany, ⁴Bioclinica Inc., Kaiser Wilhelm Str. 89, Hamburg 20355, Germany, ⁵Erwin L. Hahn Institute for Magnetic Resonance Imaging, University Duisburg-Essen, Kokereiallee 7, Essen 45141, Germany, ⁶High-Field and Hybrid MR Imaging, University Hospital Essen, Hufelandstraße 55, Essen 45147, Germany

Abstract

Background Changes in muscle fat composition as for example observed in sarcopenia or muscular dystrophy affect physical performance and muscular function, like strength and power. The purpose of the present study is to measure the repeatability of Dixon magnetic resonance imaging (MRI) for assessing muscle volume and fat in the thigh. Furthermore, repeatability of magnetic resonance spectroscopy (MRS) for assessing muscle fat is determined.

Methods A prototype 6-point Dixon MRI method was used to measure muscle volume and muscle proton density fat fraction (PDFF) in the left thigh. PDFF was measured in musculus semitendinosus of the left thigh with a T2-corrected multi-echo MRS method. For the determination of short-term repeatability (consecutive examinations), the root mean square coefficients of variation of Dixon MRI and MRS data of 23 young and healthy (29 ± 5 years) and 24 elderly men with sarcopenia (78 ± 5 years) were calculated. For the estimation of the long-term repeatability (13 weeks between examinations), the root mean square coefficients of variation of MRI data of seven young and healthy (31 ± 7 years) and 23 elderly sarcopenic men (76 ± 5 years) were calculated. Long-term repeatability of MRS was not determined.

Results Short-term errors of Dixon MRI volume measurement were between 1.2% and 1.5%, between 2.1% and 1.6% for Dixon MRI PDFF measurement, and between 9.0% and 15.3% for MRS. Because of the high short-term repeatability errors of MRS, long-term errors were not determined. Long-term errors of MRI volume measurement were between 1.9% and 4.0% and of Dixon MRI PDFF measurement between 2.1% and 4.2%.

Conclusions The high degree of repeatability of volume and PDFF Dixon MRI supports its use to predict future mobility impairment and measures the success of therapeutic interventions, for example, in sarcopenia in aging populations and muscular dystrophy. Because of possible inhomogeneity of fat infiltration in muscle tissue, the application of MRS for PDFF measurements in muscle is more problematic because this may result in high repeatability errors. In addition, the tissue composition within the MRS voxel may not be representative for the whole muscle.

Keywords Magnetic resonance imaging; Magnetic resonance spectroscopy; Sarcopenia; Muscle; Fat quantification; Repeatability

Received: 22 March 2018; Revised: 27 July 2018; Accepted: 7 August 2018

*Correspondence to: Alexandra Grimm, Institute of Medical Physics, Friedrich-Alexander-Universität Erlangen-Nürnberg (FAU), Henkestr. 91, Erlangen 91052, Germany. Tel: +49 9131 85-25535; Fax: +49 9131 8522824, Email: alexandra.grimm@fau.de

Introduction

There is increasing evidence that muscle fat infiltration is an important factor to understand reduced mobility, for example, in elderly sarcopenic as well as in young sedentary subjects or in muscular dystrophy.^{1–5} An increase of muscle fat content changes the structural muscle composition, decreases storage of elastic energy, and increases stiffness of the muscle-tendon unit. As a consequence, muscle activation and physical performance decrease.^{6–8} Age-related or injury-related inactivity or limited mobility leads to increased muscle fat infiltration, eventually causing muscle dysfunction, which might then further increase fat infiltration.^{9,10} It is interesting that in elderly subjects, muscle mass declines at a slower rate than strength, emphasizing a strong role of muscle fat infiltration and potentially of the amount of perimuscular fat. A number of diagnostic techniques mostly based on magnetic resonance imaging (MRI) have been introduced^{11–14} for the assessment of fat. In the present study, multi-point T_2^* -corrected Dixon MRI and multi-echo T_2 -corrected magnetic resonance spectroscopy (MRS) were used to measure proton density fat fraction (PDFF) and proton density water fraction (PDWF) while minimizing MR-specific effects.

For monitoring age-related, disease-related, and treatment-related effects, the precision of the technique to determine perimuscular and intramuscular fat must be known. For longitudinal measurements, repeatability additionally is an important performance characteristic as it determines the minimum significant change that can be determined in an individual subject.¹⁵ In the liver, repeatability of multi-echo T_2 -corrected H^1 MRS¹⁶ and of 6-point (6pt) Dixon MRI with a multistep adaptive fitting algorithm¹⁷ has been shown. Dixon MRI is gaining importance in clinical practice as it matches the accuracy of spectroscopy but provides fat assessment with high spatial resolution.^{18–23} In muscle, a high correlation between MRS and T_2^* -corrected 6pt Dixon MRI with calibrated spectral modelling of fat^{23–25} has been shown for fat fraction measurements; however, to our knowledge in muscle, the repeatability of MRS and Dixon imaging PDFF measurements has not been investigated so far.

The purpose of the present study is to measure the short-term and long-term repeatability of T_2^* -corrected 6pt Dixon MRI with calibrated spectral modelling of fat for assessing muscle volume and fat. Furthermore, short-term repeatability of multi-echo T_2 -corrected MRS for assessing muscle fat was determined. Both measurements were performed in young healthy and in elderly sarcopenic subjects.

Materials and methods

Subject population

Short-term repeatability (consecutive examinations) was determined in 23 young healthy men (29 ± 5 years) (G1) and

in 24 elderly men (78 ± 5 years) with sarcopenia (G2). Long-term repeatability (13-week-period between examinations) was determined in seven young and healthy men (31 ± 7 years) (G3) and in 23 elderly men (76 ± 5 years) with sarcopenic obesity (G4). All seven subjects of G3 were also subjects of the short-term group G1. Eight subjects of G4 were also subjects of the short-term group G2. Inclusion criteria for G1 was the absence of severe medical conditions and at least 3 h of physical training per week for at least 6 months prior to study enrolment. Inclusion criteria for the elderly subjects (G2 and G4) were a skeletal muscle mass index $<7.71 \text{ kg/m}^2$ and a body fat percentage $>27\%$ as measured by bioelectrical impedance analysis (InBody 770, Seoul, Korea). The young subjects (G1 and G3) were used as healthy controls. The subject groups were chosen to cover a wide range of possible fat contents to validate the method.

The study was approved by the local ethical review committee and was therefore performed in accordance with the ethical standards laid down in the 1964 Declaration of Helsinki and its later amendments. Written informed consent was obtained from each subject prior to examination.

Magnetic resonance data acquisition and magnetic resonance examination

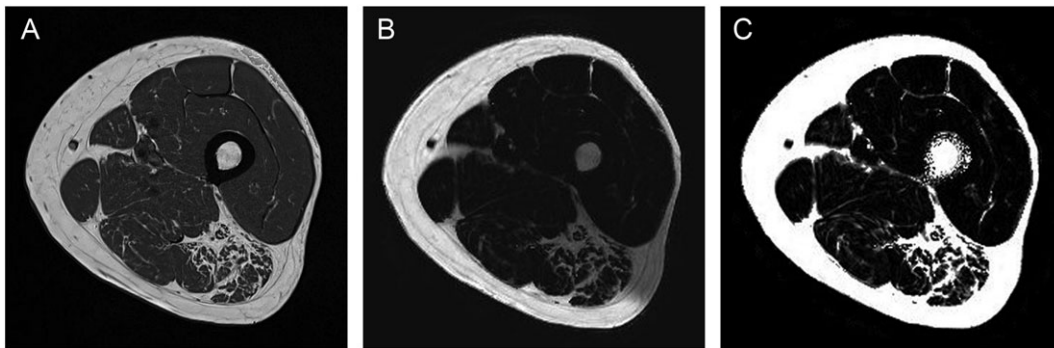
Magnetic resonance imaging sequences

Repeatability was determined for a 6pt Dixon and an MRS sequence. Additionally, the protocol included a clinically common T_1 -weighted (T_1w) turbo spin echo sequence for high-resolution anatomical reference (sequence parameter: image resolution: $0.5 \times 0.5 \times 3.0 \text{ mm}^3$; slices: 34; matrix size: 512×512 ; TR: 844 ms; echo time (TE): 14 ms; bandwidth: 488 Hz/px; acquisition time: 2:54 min). Exemplary T_1w , Dixon fat, and Dixon PDFF images of an elderly subject are shown in *Figure 1*.

The Dixon sequence was a Gradient Echo Volumetric Interpolated Breathhold Examination 6pt Dixon prototype sequence (sequence parameter: image resolution: $0.8 \times 0.8 \times 3.0 \text{ mm}^3$; slices: 36, no spacing between slices; matrix size: 320×320 ; TR: 14.00 ms; TEs: 1.90, 3.73, 5.56, 7.39, 9.22, and 11.05 ms; bandwidth: 710 Hz/px; acquisition time: 1:17 min). Minimum possible TE values were selected at the given image resolution as validated previously.²⁵ T_2^* -decay was considered as a degree of freedom in the parameter extraction, and the effect on the extracted water and fat signals was eliminated using a multi-step fitting approach.²³ From the 6pt Dixon sequence, PDFF and PDWF maps were obtained. A time-domain calibration of the fat signal dephasing optimized for liver applications was used.²⁴

The spectroscopy method for PDFF measurements was a high-speed T_2 -corrected multi-echo (HISTO) H^1 MRS (sequence parameter: voxel size: $15 \times 15 \times 15 \text{ mm}^3$; TR: 3000 ms; TEs: 12, 24, 36, 48, and 72 ms; bandwidth:

Figure 1 (A) T1w, (B) Dixon fat, and (C) Dixon proton density fat fraction images of an elderly subject (74 years, G2 and G4).



1200 Hz/px; acquisition time: 0:15 min). The positioning of the spectroscopy voxel is visualized in *Figure 2*.

Magnetic resonance examination

All subjects were examined at the mid-level of the left thigh. Axial slices were obtained using a 3-Tesla MR system (MAGNETOM Skyra^{fit}, Siemens Healthcare GmbH, Erlangen, Germany). Subjects were positioned in supine position with feet first towards the MR system. Data acquisition was performed by using a flexible 18-channel body radiofrequency (RF) surface coil for signal reception. For best signal homogeneity in the volume of interest, the flexible surface RF coil was wrapped around the mid-level of the thigh. MRS was performed in the semitendinosus muscle, which is part of the hamstring muscle group. Semitendinosus was chosen because it could be separated well from surrounding muscles and was large enough to encompass the entire MRS voxel ($15 \times 15 \times 15 \text{ mm}^3$) in all subjects. The voxel was positioned in regions without macroscopic fatty septa, if possible.

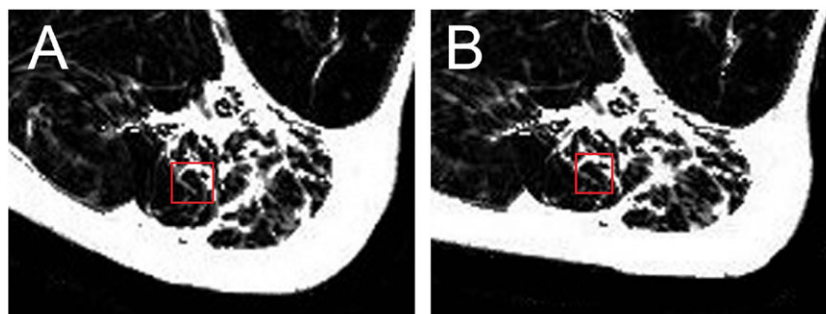
For determination of short-term repeatability, two measurements of the 6pt prototype Dixon sequence were

acquired (M1 and M2). Measurement M2 was acquired after removing the flexible RF coil from the thigh and repositioning of the subject. Additionally, all MR system adjustments that included shimming and localization were repeated for M2. MRS was measured three times, first with repositioning between M1 and M2 and then a third time without repositioning the subject or the spectroscopy volume (M3).

For determination of long-term repeatability, the MR measurements (T1w turbo spin echo and 6pt Dixon) were repeated after 13 weeks (M4). Subjects maintained their usual physical activity between the examinations. Physical activity was monitored by a questionnaire addressing training frequency, intensity, and volume. Long-term repeatability was not determined for MRS.

To standardize the location of data acquisition, the subject-specific length between the top edge of the patella and the iliac crest was measured before the first measurement. For each measurement, the acquired volume of interest was centred at half the length measured between the top edge of the patella and the iliac crest.

Figure 2 Position of magnetic resonance spectroscopy (MRS) voxel (A) before and (B) after subject repositioning in the subject shown in Figure 1. The two images demonstrate the challenge to reposition subject and MRS voxel. Muscle is elastic and easily deforms during repositioning. An inhomogeneous fat infiltration as shown here further complicates exact repositioning.



Magnetic resonance data post-processing

Manual segmentation of the fascia of the thigh muscle was performed in the prototype 6pt Dixon PDF maps. For M1, the central five slices of the stack consisting of 36 images were analysed. For M2 and M4, the corresponding slices were selected manually. Veins were used as landmarks for orientation. T₁w images were used to support the identification of the fascia. The femoral bone was excluded from the segmentation mask. Exemplary segmentation masks are shown in Figure 3. The segmentation masks were used to calculate PDWF and PDFF within the fascia, that is, the analysed volume included all muscular and perimuscular fat. By definition, PDFF and PDWF add up to one. Volume of muscle tissue (MT) was estimated as volume inside the fascia multiplied by PDWF. The repeatability analysis was carried out for the average PDFF of the entire segmentation masks of the central five slices of the intrafascia volume measured in percent and for estimated MT volume measured in cm³.

Statistical analysis

Short-term and long-term repeatability was determined as root mean square coefficient of variation (CV_{RMS})¹⁵ in percent (%). The least significant change (LSC) was determined as $2.77 \times CV_{RMS}$. If results from two measurements of an individual differ by more than the LSC with 95% confidence, a true change occurred.²⁶ As appropriate, paired or unpaired *t*-tests were carried out to compare the differences between the visits or the groups. A *P*-value of <0.05 was considered statistically significant. All statistical analyses were carried out with IBM SPSS I Statistics version 23.

Results

All 62 subjects could be examined successfully and repeatedly. The fascia was visible on the T₁w and the Dixon fat

images, but not on the PDFF map. Still, with the guidance of the T₁w images serving as anatomical reference, manual segmentation of the PDFF maps could be performed in all subjects. The MRS examination was more challenging as the positioning of the muscles differed between both measurements (M1 and M2). An exemplary case is shown in Figure 2.

Proton density fat fraction measurements

The group averages of estimated MT volume and PDFF are given in Table 1. At M1, differences in estimated MT volume and PDFF were not statistically significant between the young subjects of groups G1 and G3 ($P > 0.2$ for both parameters) nor between the elderly subjects of group G2 and G4 ($P > 0.7$ for both parameters). Longitudinally, in G4, PDFF was 4.9% higher for M4 compared with M1 ($P = 0.0003$). For all other measurements, no significant differences were detected between M1 and M4 measurements.

Repeatability

Short-term repeatability (CV_{RMS}) errors of PDFF and estimated MT volume from Dixon imaging and PDFF from MRS are given in Table 2 along with resulting LSC values. The short-term repeatability error was below 2% for all parameters obtained from Dixon imaging. In comparison, all MRS short-term repeatability errors were larger than 9%. MRS PDFF errors were significantly higher after repositioning in the young subjects ($P < 0.04$).

Long-term repeatability errors that were only determined for Dixon imaging are given in Table 3. For the elderly subjects, the long-term repeatability error for estimated muscle PDFF was significant larger than the short-term error ($P < 0.03$).

Figure 3 Dixon proton density fat fraction maps of the (A) first (M1) and (B) second (M2) measurement as well as (C) the (M4) after 13 weeks with the corresponding segmentation masks of the subject shown in Figure 1.

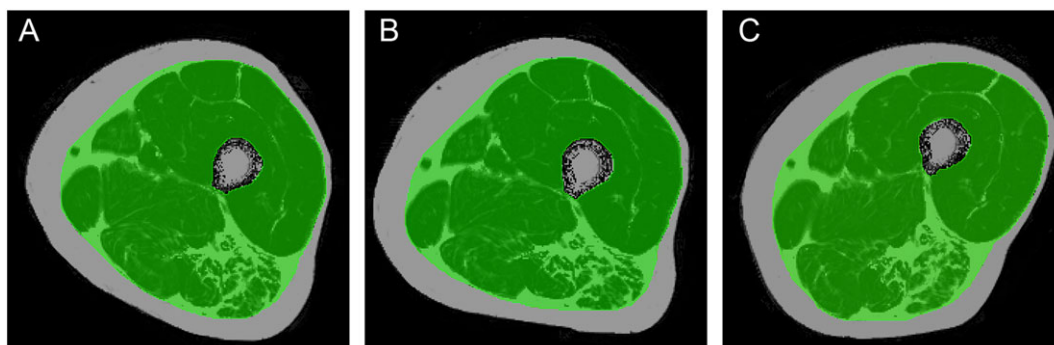


Table 1. Group averages (mean value ± SD) from Dixon magnetic resonance imaging measurement of estimated muscle tissue volume and proton density fat fraction within the fascia of the first (M1) and second (M2) measurement used to determine short-term repeatability

Group	Estimated MT volume [cm ³]			PDFF [%]		
	M1	M2	M4	M1	M2	M4
G1 n = 23	250 ± 32	245 ± 26	—	6.9 ± 2.4	6.6 ± 1.8	—
G3 n = 7	253 ± 38	244 ± 20	257 ± 22	5.7 ± 1.4	5.6 ± 1.3	5.6 ± 1.4
G2 n = 24	160 ± 21	159 ± 22	—	19.3 ± 6.0	19.1 ± 6.2	—
G4 n = 23	160 ± 21	—	161 ± 22	18.6 ± 6.0	—	19.4 ± 6.1 ^a

Long-term repeatability was determined from measurements M1 and M4 (13 weeks apart). G1: young, short-term; G3: young, long-term; G2: elderly, short-term; G4: elderly, long-term groups. MT, muscle tissue; PDFF, proton density fat fraction.

^aSignificant difference between M1 and M4 results.

Discussion

In this study, short-term and long-term repeatability of estimated MT volume and intrafascia PDFF in young and elderly subjects using Dixon MRI and MRS were measured. According to the knowledge of the authors, this is the first repeatability study of MRI and MRS for fat and muscle measurements in the thigh. Repeatability is an important performance characteristic. It determines the LSC that can be determined with a single measurement in an individual subject.²⁷ Repeatability is also inversely proportional to sample size an important consideration in planning studies.²⁸

In the present study, reported repeatability errors include variations caused by the subject repositioning and by the manual segmentation process. Short-term repeatability errors of Dixon imaging were excellent (below 2% for both parameters in young and in elderly subjects). This shows an impressive stability of the complete imaging acquisition and processing workflow. For DXA, the current gold standards of soft tissue composition assessments, *in vivo* short-term repeatability errors of whole body fat mass of around 1% to

2.3% and of lean mass of around 0.5% to 1%, have been reported.^{29,30} However, in the MR measurements of the present study, the investigated volume was much smaller. Published short-term repeatability errors of regional DXA measurements, for example, of the legs or arm of 2.5% to 5.6% were comparable with or higher than the Dixon MRI results observed in this study.^{30–32}

Short-term errors of MRS PDFF with values between 9.0% and 15.3% were much higher than those of MRI. This can be attributed to two reasons. Firstly, the MRS voxel is much smaller than the intrafascia volume analysed for the Dixon images. Thus, an inhomogeneous fat distribution as demonstrated in *Figure 2* has a much larger effect on precision if only a small volume is analysed. Secondly, muscle is a flexible tissue that deforms easily between measurements. Therefore, the exact repositioning of the MRS voxel in muscle is challenging, and also, slight motion caused by involuntary muscle contraction or relaxation will influence the content of the measured volume. This is in particular a problem in case of an inhomogeneous fat infiltration as shown in *Figure 2*. Because of the high short-term repeatability errors of MRS, long-term errors were not determined for MRS.

In rather homogeneous liver tissue for which MRS has been developed originally, MRS repeatability errors are smaller. Pineda *et al.*¹⁶ reported a reproducibility of HISTO PDFF measurements in the liver and found a CV_{RMS} of 6.4% (three separate sessions, three measurements per session,

Table 2. Short-term repeatability given as root mean square coefficient of variation with the corresponding least significant change in parentheses

Group	Dixon MRI		MRS	
	Estimated MT volume [%]	PDFF [%]	PDFF [%] without repositioning	PDFF [%] with repositioning
G1 n = 23	1.2 (3.3)	2.1 (5.8)	9.3 (25.8)	15.3 ^a (42.4)
G2 n = 24	1.5 (4.2)	1.6 (4.4)	11.1 (30.7)	9.0 (24.9)

Left: root mean square coefficient of variation (CV_{RMS}) of estimated muscle tissue (MT) volume and proton density fat fraction (PDFF) obtained from Dixon imaging include repositioning. Right: MRS CV_{RMS} were only determined for PDFF. G1: young, short-term; G2: elderly, short-term group. MRI, magnetic resonance imaging; MRS, magnetic resonance spectroscopy.

^aSignificant higher errors with repositioning.

Table 3. Long-term repeatability given as root mean square coefficient of variation of estimated muscle tissue (MT) volume and proton density fat fraction (PDFF) obtained from Dixon imaging

Group	Estimated MT volume [%]	PDFF [%]
G3 n = 7	4.0	2.1
G4 n = 23	1.9	4.2 ^a

The two measurements were 13 weeks apart. G3: young, long-term; G4: elderly, long-term group. MT, muscle tissue; PDFF, proton density fat fraction.

^aSignificant higher error than in short-term repeatability (Table 2).

three subjects). Usually, spatial variations of liver tissue and of liver fat are small. MRS of muscle is more complicated because adipose tissue infiltrations lead to an inhomogeneous tissue composition in the captured MRS voxel. Larger amounts of fatty septa can lead to errors in the MRS fat measurement. Especially in the elderly subjects of our study, it was not always possible to position the MRS voxel in homogeneous MT volumes without macroscopic fatty septa. This may explain why the repeatability error in MRS was also high without subject and voxel repositioning. Reproducibility will be higher in muscles or other tissues with a more homogeneous fat distribution. This explains why MRS is successfully used to determine liver fat. Another reason for an increased variability of PDFF results could be an imprecise voxel excitation by the RF pulse or the extrapolation of fat and water signals at five successive ETs to TE equals zero for T₂-correction. Because of the inhomogeneous fat distribution in muscle, the tissue composition within the MRS voxel may also not be representative for the whole muscle.

A potential limitation of the MRS measurement in the present study was the positioning of the subjects. Legs were positioned flat on the scanner table, potentially increasing the degree of muscle deformation. Elevated and cushion-supported knees might have prevented deformation changes between measurements and could potentially decrease repeatability errors of MRS. However, a pre-investigation showed that this position was less endurable for most subjects and, in consequence, caused more movement artefacts especially in elderly subjects.

Long-term repeatability was only determined for MRI Dixon imaging, but not for MRS. CV_{RMS}-values were lower than 4.2% (Table 3). As expected, long-term errors were slightly higher than short-term errors, but the direct comparison of the long-term and short-term errors is difficult as is the comparison of the results within Table 3. This has a number of reasons. First, the group size of G3 (young subjects) was much smaller than G4 (elderly subjects). Some but not all subjects were included in the short-term and long-term analysis. More importantly, the long-term assessment included physiological changes that cannot be separated. Therefore, LSC values are only given for short-term repeatability. Still, an upper limit and the statement that long-term repeatability of estimated MT volume and PDFF was better than 4% can be given. An important factor that should not be neglected in long-term muscle measurements is hydration that can vary between the visits.^{33,34} In the subjects examined in the present study, a significant difference (paired *t*-test, *P* > 0.05) of total body water per body weight (body water percentage) was observed.

From experience, one would speculate that repeatability errors were greater in elderly subjects because of higher amounts of muscle fat and lower MT volume (Table 1). Furthermore, the variance within the groups was not higher in the elderly compared with the young groups (Table 1). A typically larger variation in elderly subjects is an important argument to determine

a technique's repeatability not only in young healthy but also in elderly subjects.¹⁵ Finally, higher hydration states in follow-up measurements would cause a fat underestimation and vice versa. Given these limitations, the long-term and short-term repeatability results of our study fit together well.

The LSC is an important performance criterion of a technique because it determines the minimum change in an individual that can be considered significant. LSC values for Dixon parameters were below 6% (Table 2). Reported longitudinal changes of adipose tissue within muscles in humans are rare. In young (19–28 years) subjects, Manini *et al.* reported a 14.5% increase in IMAT (combination of perimuscular and intramuscular adipose tissue within the fascia) of the thigh and a 20% increase in IMAT of the calf after 4 weeks of lower-limb suspension as measured in T₁w MRI images.¹⁰ In elderly subjects (70–79 years), Delmonico *et al.* determined the 5-year age-related changes of IMAT in the thigh with computed tomography and reported an increase of 29.0 ± 43.6% in women and of 48.5 ± 59.6% in men (mean value ± SD).³⁵ PDFF changes after a 13-week physical training with 6pt Dixon MRI (so far unpublished data) were measured in a study parallel to the present one. A decrease of 13.1% ± 8.2% and of 1.6% ± 3.6% (mean value ± SD) in young (*n* = 11) and elderly (*n* = 27) subjects was found, respectively. Thus, for the majority of these longitudinal measurements, the repeatability errors of the Dixon MRI used in this study are sufficiently low. In comparison, long-term repeatability errors reported for DXA body composition measurements were 2.0% for total body, 6.0% for arms, and 3.0% for legs.³⁰

So far, most studies in cachexia and sarcopenia focus on body composition measured by DXA or bioelectrical impedance analysis, on muscle size, and more rarely on adipose tissue, usually either measured in T1-weighted MR images as volume of fatty infiltration or as CT density in Hounsfield units.³⁶ Correlation of lean tissue values or muscle size with functional muscle measures is usually weak.^{37–40} Shifting the focus towards infiltration of muscle by adipose tissue and the distribution of adipose tissue within muscle will probably improve the understanding of pathophysiological processes and the mechanism of interventions. Our results show that compared with standard methods, there is no 'repeatability penalty' using MR Dixon imaging to quantify PDFF. LSC in individual patients and sample sizes of studies will not increase, and this advanced imaging method could easily be integrated in existing study designs.

The image processing part in this study has limitations. So far, no robust automatic image segmentation has been developed. Therefore, only five of the acquired 36 slices were used for the analysis, which might cause an overestimation of the repeatability errors compared with a possible three-dimensional analysis of the whole thigh muscle. The manual segmentation may have further increased errors because of intra-observer variability. Furthermore, only the fascia but not the muscles was segmented; thus, PDFF within muscles was

not determined separately. From a medical perspective, subcutaneous, perimuscular, and intramuscular adipose tissue should be assessed separately,^{1,4,9,35,41–44} because intramuscular fat is known to have the strongest effect on decreasing functional performance and muscle function.^{3,6} This requires a separate segmentation of individual muscles and of the perimuscular fat, which is still a work in progress. Precision errors in individual muscle may increase compared with the numbers presented in *Tables 2* and *3* because the volume is smaller.

In conclusion, PDFF and muscle volume can be measured with excellent repeatability by T_2^* -corrected 6pt Dixon MRI with calibrated spectral modelling of fat in young and elderly subjects. LSCs of below 6% seem to be adequate to monitor disease or intervention-related changes as reported in the literature. This supports the use of multi-point Dixon MRI to predict potential future mobility impairments or measure the success of a therapeutic intervention addressing muscle function in aging populations and in muscular dystrophy. The application of MRS for PDFF measurements in muscle is more problematic because the large inhomogeneity of MT due to fat infiltration results in high repeatability errors. In addition, the tissue composition within the MRS voxel may not be representative for the whole muscle.

Acknowledgements

The authors certify that they comply with the ethical guidelines for authorship and publishing of the *Journal of Cachexia, Sarcopenia, and Muscle*⁴⁵.

References

- Hilton TN, Tuttle LJ, Bohnert KL, Mueller MJ, Sinacore DR. Excessive adipose tissue infiltration in skeletal muscle in individuals with obesity, diabetes mellitus, and peripheral neuropathy: association with performance and function. *Phys Ther* 2008; **88**:1336–1344.
- Kallman DA, Plato CC, Tobin JD. The role of muscle loss in the age-related decline of grip strength. *J Gerontol* 1990; **45**:M82–M88.
- Marcus RL, Addison O, Dibble LE, Foreman KB, Morrell G, Lastayo P. Intramuscular adipose tissue, sarcopenia, and mobility function in older individuals. *J Aging Res* 2012; **2012**:629–637.
- Tuttle LJ, Sinacore DR, Mueller MJ. Intermuscular adipose tissue is muscle specific and associated with poor functional performance. *J Aging Res* 2012; **2012**:172957.
- Visser M, Goodpaster BH, Kritchevsky SB, Newman AB, Nevitt M, Rubin SM, et al. Muscle mass, muscle strength, and muscle fat infiltration as predictors of incident mobility limitations in well-functioning older persons. *J Gerontol* 2005; **60**:324–333.
- Robles PG, Sussman MS, Naraghi A, Brooks D, Goldstein RS, White LM, et al. Intramuscular fat infiltration contributes to impaired muscle function in COPD. *Med Sci Sports Exerc* 2015; **47**:1334–1341.
- Yoshida Y, Marcus RL, Lastayo PC. Intramuscular adipose tissue and central activation in older adults. *Muscle Nerve* 2012; **46**:813–816.
- Faria A, Gabriel R, Abrantes J, Bras R, Moreira H. Triceps-surae musculotendinous stiffness: relative differences between obese and non-obese postmenopausal women. *Clin Biomech* 2009; **24**:866–871.
- Addison O, Marcus RL, Lastayo PC, Ryan AS. Intermuscular fat: a review of the consequences and causes. *Int J Endocrinol* 2014; **2014**:ID 309570, 1, 11.
- Manini TM, Clark BC, Nalls MA, Goodpaster BH, Ploutz-Snyder LL, Harris TB. Reduced physical activity increases intermuscular adipose tissue in healthy young adults. *Am J Clin Nutr* 2007; **85**:377–385.
- Antony J, McGuinness K, Welch N, Coyle J, Franklyn-Miller A, O'Connor NE, et al. Fat quantification in MRI-defined lumbar muscles. *IEEE T Image Process* 2014; **4**:2154–512X.
- Barra V, Boire J-Y. Segmentation of fat and muscle from MR images of the thigh by a possibilistic clustering algorithm. *Comput Methods Programs Biomed* 2002; **68**:185–193.
- Orgiu S, LaFortuna CL, Rastelli F, Cadioli M, Falini A, Rizzo G. Automatic muscle and fat segmentation in the thigh from T1-Weighted MRI. *J Magn Reson Imaging* 2016; **43**:601–610.
- Yang YX, Chong MS, Tay L, Yew S, Yeo A, Tan CH. Automated assessment of thigh composition using machine learning for Dixon magnetic resonance images. *Magn Reson Mater Phys* 2016; **29**:723–731.
- Glüer CC, Blake Y, Lu Y, Blunt BA, Jergas M, Genant HK. Accurate assessment of

Conflict of interest

Co-authors Heiko Meyer, Mathias Nittka, Marcel D. Nickel, and Esther Raithel are employees of Siemens Healthcare GmbH, Erlangen, Germany. Klaus Engelke is a part-time employee of Bioclinica Hamburg, Germany. Alexandra Grimm, Oliver Chaudry, Andreas Friedberger, Michael Uder, Wolfgang Kemmler, and Harald H. Quick declare that they have no conflict of interest.

- precision errors: how to measure the reproducibility of bone densitometry techniques. *Osteoporos Int* 1995;**5**:262–270.
16. Pineda N, Sharma P, Xu Q, Hu X, Vos M, Martin DR. High-speed T2-corrected multiecho acquisition at 1H MR spectroscopy—a rapid and accurate technique. *Radiology* 2009;**252**:568–576.
 17. Sofue K, Mileto A, Dale BM, Zhong X, Bashir MR. Interexamination repeatability and spatial heterogeneity of liver iron and fat quantification using MRI-based multi-step adaptive fitting algorithm. *J Magn Reson Imaging* 2015;**42**:1281–1290.
 18. Hines CDG, Yu H, Shimakawa A, McKenzie CA, Brittain JH, Reeder SB. T1 independent, T2* corrected MRI with accurate spectral modeling for quantification of fat: validation in a fat-water-SPIO phantom. *J Magn Reson Imaging* 2009;**30**:1215–1222.
 19. Kovanlikaya A, Guclu C, Desai C, Becerra R, Gilsanz V. Fat quantification using three-point dixon technique: in vitro validation. *Acad Radiol* 2005;**12**:636–639.
 20. Noble JJ, Keevil SF, Totman J, Charles-Edwards GD. In vitro and in vivo comparison of two-, three- and four-point Dixon techniques for clinical intramuscular fat quantification at 3 T. *Br J Radiol* 2014;**87**:20130761.
 21. Reeder SB, McKenzie CA, Pineda AR, Yu H, Shimakawa A, Brau AC, et al. Water–fat separation with IDEAL gradient-echo imaging. *J Magn Reson Imaging* 2007;**25**:644–652.
 22. Bernard CP, Liney GP, Manton DJ, Turnbull LW, Langton CM. Comparison of fat quantification methods: a phantom study at 3.0T. *J Magn Reson Imaging* 2008;**27**:192–197.
 23. Zhong X, Nickel MD, Kannengiesser SAR, Dale BM, Kiefer B, Bashir MR. Liver fat quantification using a multi-step adaptive fitting approach with multi-echo GRE imaging. *Magn Reson Med* 2014;**72**:1353–1365.
 24. Nickel MD, Kannengiesser SAR, Kiefer B. Time-domain calibration of fat signal dephasing from multi-echo STEAM spectroscopy for multi-gradient-echo imaging based fat quantification. In: Proceedings of the 23rd Annual Meeting of ISMRM, Toronto, 2015.
 25. Grimm A, Meyer H, Nittka M, Nickel MD, Raithel E, Chaudry O, et al. Evaluation of 2-point, 3-point, and 6-point Dixon magnetic resonance imaging with flexible echo timing for muscle fat quantification. *Eur J Radiol* 2018;**103**:57–64.
 26. Kim H-S, Yang S-O. Quality control of DXA system and precision test of radiotechnologists. *J Bone Metab* 2014;**21**:2–7.
 27. Glüer C. Monitoring skeletal changes by radiological techniques. *J Bone Miner Res* 2009;**14**:1952–1962.
 28. Fitzmaurice G. Sample size and precision. *Nutrition* 1999;**15**:803–804.
 29. Toombs RJ, Ducher G, Shepherd JA, de Souza MJ. The impact of recent technological advances on the trueness and precision of DXA to assess body composition. *Obesity* 2012;**20**:30–39.
 30. Gorgey AS, Ciriigliaro CM, Bauman WA, Adler RA. Estimates of the precision of regional and whole body composition by dual-energy x-ray absorptiometry in persons with chronic spinal cord injury. *Spinal Cord* 2018;<https://doi.org/10.1038/s41393-018-0079-x>.
 31. Hind K, Oldroyd B. In-vivo precision of the GE Lunar iDXA densitometer for the measurement of appendicular and trunk lean and fat mass. *Eur J Clin Nutr* 2013;**67**:1331–1333.
 32. Rothney MP, Martin F-P, Xia Y, Beaumont M, Davis C, Ergun D, et al. Precision of GE Lunar iDXA for the measurement of total and regional body composition in nonobese adults. *J Clin Densitom* 2012;**15**:399–404.
 33. Olsson KE, Saltin B. Variation in total body water with muscle glycogen changes in man. *Acta Physiol Scand* 1970;**80**:11–18.
 34. Flear CT, Carpenter RG, Florence I. Variability in the water, sodium, potassium, and chloride content of human skeletal muscle. *J Clin Pathol* 1965;**18**:74–81.
 35. Delmonico MJ, Harris TB, Visser M, Park SW, Conroy MB, Velasquez-Mieyer P, et al. Longitudinal study of muscle strength, quality, and adipose tissue infiltration. *Am J Clin Nutr* 2009;**90**:1579–1585.
 36. Engelke K, Museyko O, Wang L, Laredo JD (2018 (sub)) Quantitative analysis of skeletal muscle by CT imaging—a review. *JOT*.
 37. Tournadre A, Pereira B, Dutheil F, Giraud C, Courteix D, Sapin V, et al. Changes in body composition and metabolic profile during interleukin 6 inhibition in rheumatoid arthritis. *J Cachexia Sarcopenia Muscle* 2017;**8**:639–646.
 38. Makizako H, Shimada H, Doi T, Tsutsumimoto K, Lee S, Lee CS, et al. Age-dependent changes in physical performance and body composition in community-dwelling Japanese older adults. *J Cachexia Sarcopenia Muscle* 2017;**8**:607–614.
 39. Kvorning T, Christensen LL, Madsen K, Nielsen LJ, Gejl DK, Brixen K, et al. Mechanical muscle function and lean body mass during supervised strength training and testosterone therapy in aging men with low-normal testosterone levels. *J Am Geriatr Soc* 2013;**61**:957–962.
 40. Fabbri E, Chiles Shaffer N, Gonzalez-Freire M, Shardell MD, Zoli M, Studenski SA, et al. Early body composition, but not body mass, is associated with future accelerated decline in muscle quality. *J Cachexia Sarcopenia Muscle* 2016;**8**:490–499.
 41. Machann J, Bachmann OP, Brechtel K, Dahl DB, Wietek B, Klumpp B, et al. Lipid content in the musculature of the lower leg assessed by fat selective MRI: intra- and interindividual differences and correlation with anthropometric and metabolic data. *J Magn Reson Imaging* 2003;**17**:350–357.
 42. McGregor RA, Cameron-Smith D, Poppitt SD. It is not just muscle mass: a review of muscle quality, composition and metabolism during ageing as determinants of muscle function and mobility in later life. *Longev Healthspan* 2014;**3**:9.
 43. Schaap LA, Pluijms SMF, Deeg DJH, Visser M. Inflammatory markers and loss of muscle mass (sarcopenia) and strength. *Am J Med* 2006; **119**:526.e9–17.
 44. Zoico E, Rossi A, Di Francesco V, Sepe A, Oliosio D, Pizzini F, et al. Adipose tissue infiltration in skeletal muscle of healthy elderly men: relationships with body composition, insulin resistance, and inflammation at the systemic and tissue level. *J Gerontol* 2010;**65**:295–299.
 45. von Haehling S, Morley JE, Coats AJS, Anker SD. Ethical guidelines for publishing in the Journal of Cachexia, Sarcopenia and Muscle: update 2017. *J Cachexia Sarcopenia Muscle* 2017;**8**:1081–1083.